Composites Part C: Open Access 4 (2021) 100112

Contents lists available at ScienceDirect

Composites Part C: Open Access

journal homepage: www.elsevier.com/locate/jcomc

Characterization of carbon fiber reinforced PLA composites manufactured by fused deposition modeling

Nabeel Maqsood*, Marius Rimašauskas

Department of Production Engineering, Faculty of Mechanical Engineering and Design, Kaunas University of Technology, 51424 Kaunas, Lithuania

ARTICLE INFO

Keywords:
Additive manufacturing
Fiber reinforced thermoplastic composites
Mechanical properties

ABSTRACT

Additive manufacturing (AM) is a process of producing 3D parts with complex geometries by depositing layer-by-layer and these technologies have been successfully utilized in numerous engineering application. Fused deposition modeling (FDM) is one of the most promising material extrusion based and commonly used AM technology, which is most widely used for producing thermoplastic parts for functional applications with aim of low cost, minimum wastage and simplicity of material conversion. Due to substantially inadequate mechanical performance of pure thermoplastics material, there is a need to improve the mechanical properties of FDM generated thermoplastic parts. One of the possible methods is to add the reinforcement material such as continuous carbon fiber (CCF) to the thermoplastic matrix to form continuous carbon fiber reinforced polymer composite (CCFRPC), which could be used in engineering applications. Four groups of specimens were prepared: poly-lactic acid thermoplastic (PLA), PLA with short carbon fiber (PLA-SCF), PLA printed with CCF (PLA-CCF) and PLA-SCF printed with CCF (PLA-SCF-CCF) using FDM technology. Effects on the tensile and flexural properties of specimens were experimentally investigated after FDM production process. In order to study the specimens fracture and interfacial bond of the 3D printed parts, fracture interface was observed and analyzed using optical microscope's micrograph after performing the mechanical tests.

1. Introduction

Additive manufacturing (AM) also referred as 3D printing, is an advanced process of fabricating metallic, ceramic and plastic parts and their composites with complex shape geometries [1]. AM of polymers and polymer composites have found their possible applications in various engineering industries such as aerospace and military for development of complex lightweight structures, biomedical fields for printing tissues and organs, architectural fields for structural models, automobile, construction and food processing [2,3]. Compared to conventional manufacturing techniques, AM technologies have ability to shorten the design and manufacturing cycle, thus reduce its production costs and increase competitiveness of company [4,5]. The pure polymer structures developed by AM techniques attain poor mechanical performance due to less strength and stiffness, as pure polymers have weak mechanical properties [6].

Various attempts have been made to overcome the poor mechanical performance of such printed parts. AM of polymer matrix composites with enhanced mechanical properties have resolved these limitations by introducing the reinforcements to polymer, such reinforcements include fibers or nanomaterials, forming a fiber-reinforced polymer composites (FRPCs), which are considered as high performance materials due to their exceptional functionality [2,7,8,9]. FRPCs have been intensively used in industries such as in textile [10] automobile and aerospace due to their excellent mechanical properties (high strength-to-weight ratio). Carbon, glass and aramid fibers are the most commonly reinforcements used in FRPC, which may be either continuous or discontinuous [11]. However, the composites reinforced with short fibers or particles have poor mechanical properties compared to composites reinforced with continuous fiber. The possibility of engaging continuous FRPC may lead the part with much higher mechanical performance [12].

Continuous carbon fiber-reinforced polymer composites (CCFRPCs) are lightweight and strong and can be used in a wide range of engineering applications [13,14]. Results have shown that mixing of continuous carbon fibers with polymers allows to increase composite strength, stiffness, thermal conductivity and also reduces the distortion of the parts. Moreover, such composites showed improved mechanical strength and performance compared to discontinuous carbon fiber-reinforced polymer composites (DCFRPC) [11]. CCFRPC are now becoming substitute materials to replace the conventional metals due to their excellent mechanical properties, recycling capability and potential to use as lightweight structures [15].

FDM is one of the most common and promising AM technology capable of printing FRPC functional parts having complex geometries with

* Corresponding author.
E-mail addresses: nabeel.maqsood@ktu.edu (N. Maqsood), marius.rimasauskas@ktu.lt (M. Rimašauskas).

https://doi.org/10.1016/j.jcomc.2021.100112
Received 25 November 2020; Received in revised form 6 January 2021; Accepted 18 January 2021

desirable mechanical properties [16]. FDM technique is of specific intrigued due to its relative low cost, less material utilization and ease of use [4,17]. Most of the 3D printed polymer products are still not be able to use as the functional components, since pure polymer products built by FDM have lack of strength and load-bearing properties [5,18,19]. However, FDM technology has the ability to print the polymer with the reinforcement irrespective of continuous or discontinuous depending on the nature of printing filament [20]. Previous experimental results have shown an increase in mechanical strength of CCFRPC printed through FDM process compared to pure 3D printed thermoplastic structures [2,21].

F. Ning et al. [22] studied the processability, microstructure and mechanical performance of short carbon fiber reinforced ABS composites parts fabricated by FDM and found that it can reduce the toughness, yield strength and ductility of the composites, but will increase the tensile and flexural properties. L. Love et al. [23] assessed the effects of the addition of short carbon fibers on the strength, stiffness, thermal conductivity, and distortion of FDM-fabricated parts. H. Tekinalp et al. [24] with experimental results showed that the porosity inside the FDM-printed parts increased by the addition of short carbon fiber content while voids between the beads decreased. A limited improvement in the mechanical performance has been achieved up to 20% increase in the tensile strength by the addition of short fiber due to the limitations in the reinforcement of short fiber [25]. Most of the studies have been focused on the development, fabricating and characterizing of AM of composites with short carbon fiber reinforcements and only few with continuous fiber reinforcements [2,4,17].

C. Yang [26] proposed a novel FDM process for CFRPC using continuous carbon fiber as reinforcing phase and ABS as matrix and experimental showed that flexural strength and modulus is almost six times higher than the conventional FDM ABS samples, and three times than injection molded samples. J.M. Chacón et al. [17] examined the characterization and valuation of the effect of build orientation, layer thickness and fiber volume content on the mechanical properties of 3D printed CCFRPC. Z. Hou et al. [27] proposed a design method of continuous fiber reinforced heterogeneous composites and achieved the flexural strength of the 207 MPa. T. Yu et al. [11] studied the properties and mechanical performance using CCF as reinforcement with the Onyx filament as matrix. A. Dickson et al. [5] evaluated the performance of nylon filament with CCF composites and found the tensile strength 6.3 times higher than that of the non-reinforced nylon polymer. M. Rimasauskas et al. [28] investigated tensile strength of continuous impregnated carbon fiber (1K and 3K) with polymer filaments and experimental results showed that PLA reinforced with the CCF tow impregnated with 10% wt. PLA solution has highest tensile strength of 165 MPa (3K carbon tow). M. Heidari-Rarani et al. [29] prepared 1K carbon fiber roving and printed with PLA forming CCFRPC using FDM technology with the modification in the extruder design and achieved maximum tensile and bending strength of 61.4 MPa and 152.1MPa, respectively that shows increase in the strength up to 35% and 108%, respectively compared to pure PLA.

However, few research has been reported on characterizing the failure mode and tensile and flexural behaviors of additively manufactured CCFRPC [11]. This paper aims to study the mechanical performance of PLA filament (pure and with SCF) reinforced with continuous carbon fiber and presents a comprehensive tensile and flexural response of CCFRPC and to investigate the fracture interface after performing the mechanical testing through optical microscope which has not been discussed before.

2. Experimental

2.1. Materials

In the present research, commercially available PolyLite PLA (Polymaker) and XT-CF20 (ColorFabb) 3D printing filaments having diameter of 1.75 mm were used as a matrix material. ColorFabb XT-CF20 is a filament made from PLA with short carbon fibers (PLA-SCF) of 20% carbon fiber content having flexural modulus and tensile strength of 6.2 GPa and 76 MPa, respectively (molded specimen). Continuous carbon fiber tow T300B-3000 (3000 fibers in a tow) from Toray was selected as reinforcement material having diameter of one fiber equal to 7 micrometers. T300B is a high-performance carbon fiber made of polyacrylonitrile having tensile strength, Young's modulus and density of 3530 MPa, 230 GPa and of 1.76 g/cm^3, respectively [30]. PLA 3D850 biopolymer from NatureWorks was used to impregnate carbon fiber tow having tensile strength, Young's modulus and density of 51 MPa, 2315 MPa and 1.24 g/cm^3, respectively [28]. Solvent methylene chloride (CH_2Cl_2) from Eurochemicals was used. Information of all materials concerning the mechanical properties or chemical composition were provided by materials suppliers.

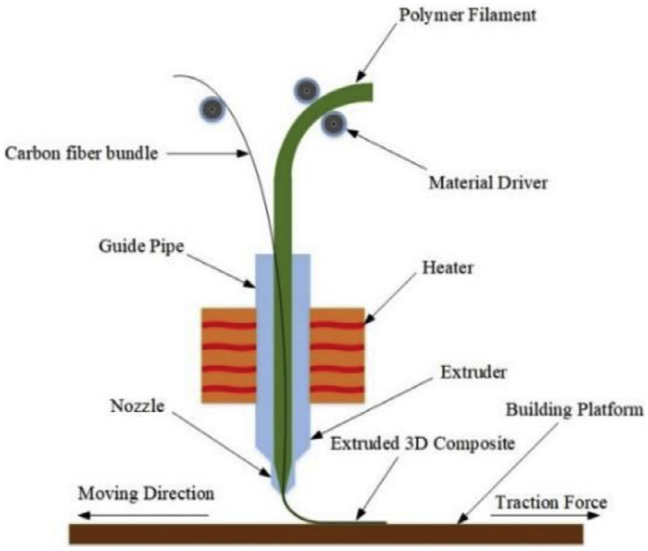

Fig. 1. Schematic view of the 3D printing of PLA reinforced with continuous carbon fiber.

2.2. Processing of impregnated carbon fiber

For the processing and preparation of impregnated carbon fiber, the same method was followed as discussed previously [28] by the author, but performed with some modifications in the process. Nozzle diameters for each part were modified for the impregnation process. Dichloromethane was used as a solvent to dissolve PLA 3D850 thermoplastic used in the form of pellets. The solution of Dichloromethane and PLA pellets was prepared with the ratio concentration of 90g/10g respectively. Thermoplastic pellets were fully dissolved by using the magnetic LBX H01 mini-stirrer at 600-rpm and during the dissolution the heating was not supplied.

2.3. Printing and process parameters

For modeling specimen geometry Pro-engineer Wildfire 5.0 software was used, then model was exported as an STL file from the software and imported to the 3D printing software for printing preparation. Modified MeCreator 2 (Geeetech) 3D printer was used for the production of PLA and PLA-SCF specimens reinforced with continuous carbon fiber (CCF), while Prusa i3 MK3S 3D printer was used to print pure PLA and PLA-SCF specimens. The printers were selected because of its simplicity and ease of use. A schematic view of the designed extrusion device to print CCFRP is presented in Fig. 1. For the printing of specimens with CCF, PLA and PLA-SCF filaments having diameters of 1.75 mm is fed to the printing head through the PTFE tube using standard filament feeding

Table 1
Parameters of 3D printing.

Parameters	3D Printers types MeCreator 2 PLA-CCF	PLA-SCF-CCF	Prusa i3 MK3S PLA	PLA-SCF
Nozzle Diameter	1.5 mm	1.5 mm	0.4 mm	0.4 mm
Extrusion Multiplier	0.5	0.5	1	1
Extrusion width	1.5 mm	1.5 mm	0.45 mm	0.45 mm
Layer height	0.5 mm	0.5 mm	0.2 mm	0.2 mm
Printing Speed	3.0 mm/s	3.0 mm/s	25 mm/s	25 mm/s
First layer speed	1.20 mm/s	1.20 mm/s	20 mm/s	20 mm/s
Extruder temperature	210^{O}C	250^{O}C	210^{O}C	250^{O}C
Bed temperature	90^{O}C	90^{O}C	60^{O}C	75^{O}C
Fan Speed	60%	60%	30%	30%
Internal/External fill pattern	Rectilinear	Rectilinear	Rectilinear	Rectilinear
Infill percentage	100%	100%	100%	100%

Table 2
Dimensions of 3D printed specimens.

Material	Tensile test Length, mm	Width, mm	Thickness, mm	Mass, g	Flexural test Length, mm	Width, mm	Thickness, mm	Mass, g
PLA	149.68 ± 0.08	13.07 ± 0.05	3.01 ± 0.04	6.80 ± 0.02	122.80 ± 0.06	12.95 ± 0.14	3.03 ± 0.08	5.56 ± 0.01
PLA-CCF	149.53 ± 0.34	12.05 ± 0.07	3.19 ± 0.02	5.58 ± 0.03	121.83 ± 0.06	12 ± 0.11	3.72 ± 0.06	5.17 ± 0.04
PLA-SCF	149.9 ± 0.07	13.04 ± 0.03	3.03 ± 0.04	6.95 ± 0.02	122.95 ± 0.03	12.96 ± 0.02	3.21 ± 0.02	5.91 ± 0.02
PLA-SCF-CCF	150.63 ± 0.23	11.91 ± 0.14	3.25 ± 0.11	5.73 ± 0.08	120 ± 0.92	11.97 ± 0.01	3.72 ± 0.05	5.14 ± 0.04

system. The heat was provided to the filaments in the printing head up to 210 ˚C for PLA and 250 ˚C for PLA-SCF, where the polymer liquefies.

Impregnated carbon fiber tow is also inserted to printing head, directly to the printing nozzle. After passing through the printing head, the polymer liquefies in the mixing zone, where molten polymer makes a bond with impregnated CCF and form a composite. The CCF tow is feeded only with the help of molten polymer, where it is constantly pushed with the molten polymer through the printing nozzle. The PLA material reinforced with carbon fiber is extruded through the printing nozzle on the borosilicate glass printing bed that is mounted on the aluminum plate.

In this study, unidirectional 0˚ flat specimens were selected to print for the experiments and isotropic fiber patterns were analyzed. Stainless steel nozzle having the diameter of 1.5 mm was used. The same process was used to print PLA and PLA-SCF specimens with standard Prusa i3 MK3S 3D printer.

All the printing parameters and dimensions of 3D printed specimens are presented in Tables 1 and 2, respectively. The samples fabrication and testing procedures are presented in Fig. 2.

The approximately carbon fiber content in the matrix was calculated by the length of tool path of the specimen. Thus, carbon fiber content measured can be considered as the weight ratio of carbon fiber to composite specimen [25]. The total number of layers and lines in layer were 6 and 7, respectively. From the scheming, approximately 18.2% and 21.8% carbon fiber content was calculated for the prepared PLA-CCF and PLA-SCF-CCF composite part structures, respectively. It is worth to mention that CF content coming from short fiber reinforced filament (XT-CF20) was not included in the calculations.

2.4. Tensile and flexural testing measurement procedures

Mechanical properties were carried out to analyze and determine the properties of 3D printed specimens. There are no standard test methods defined for determining the tensile and flexural properties of CFRPC parts fabricated using FDM technology [17]. In this study, ASTM D3039 and D790 standards were used to perform tensile and flexural testing of the specimens, respectively. According to the above-mentioned standards, five samples for each group were prepared to determine the material properties and 40 specimens in total were printed for the testing.

For the tensile testing, rectangular cross-section shape specimens with dimensions of 150 × 13 × 3 mm with the use of PLA tabs having dimensions of 50 × 12.5 × 2 mm with the bevel angle of 30^{O} were 3D printed. Four points were marked 15 mm from the center on the specimens in order to measure the elastic strain. Dual column Tinius Olsen H25KT (capacity 25 kN) universal testing machine was used to perform the test with the standard head displacement rate of 2 mm/min. The tensile strength and modulus of elasticity was calculated using the Eqs. (1) and (2), respectively.

$$F_{tu} = \frac{P_{max}}{A} \tag{1}$$

where, F_{tu} = ultimate tensile strength (MPa), P_{max} = maximum load before failure (N), A = average cross-sectional area (mm^2).

$$E = \frac{\Delta\sigma}{\Delta \in} \tag{2}$$

where, E = modulus of elasticity (GPa), $\Delta\sigma$ = difference in applied tensile stress between two strain points, $\Delta \in$ = difference between the two strain points.

For the flexural testing, the specimens were fabricated with dimensions of 123 × 12.7 × 3.2 mm. According to the standard 5 samples were prepared for each group to perform the test to obtain an average value of the targeted properties. Three-point bending set-up (two supports and one midway load nose each of 10mm diameter) was prepared for the flexural test using Tinius Olsen H25KT universal testing machine. The test was performed using the rate of crosshead motion of 1.35 mm/min with the span support length of 51.2 mm. Data acquisition software (Tinius Olsen Horizon) was used to collect the force (N) and displacement (mm) relationships. The flexural stress and flexural modulus of elasticity was calculated using the Eqs. (3) and (4), respectively.

$$\sigma_f = \frac{3PL}{2bd^2} \tag{3}$$

where, σ_f = flexural stress, P = load at a given point on the load-deflection curve (N), L = support span length (mm), b = width of tested specimen (mm), d = depth of tested specimen (mm).

$$E_f = \frac{(\sigma_{f2} - \sigma_{f1})}{(\in_{f2} - \in_{f1})} \tag{4}$$

where, E_f = flexural modulus, σ_{f2} and σ_{f1} = flexural stresses at the predefined points on the load deflection curve, $\in_{f2}$ and $\in_{f1}$ = flexural

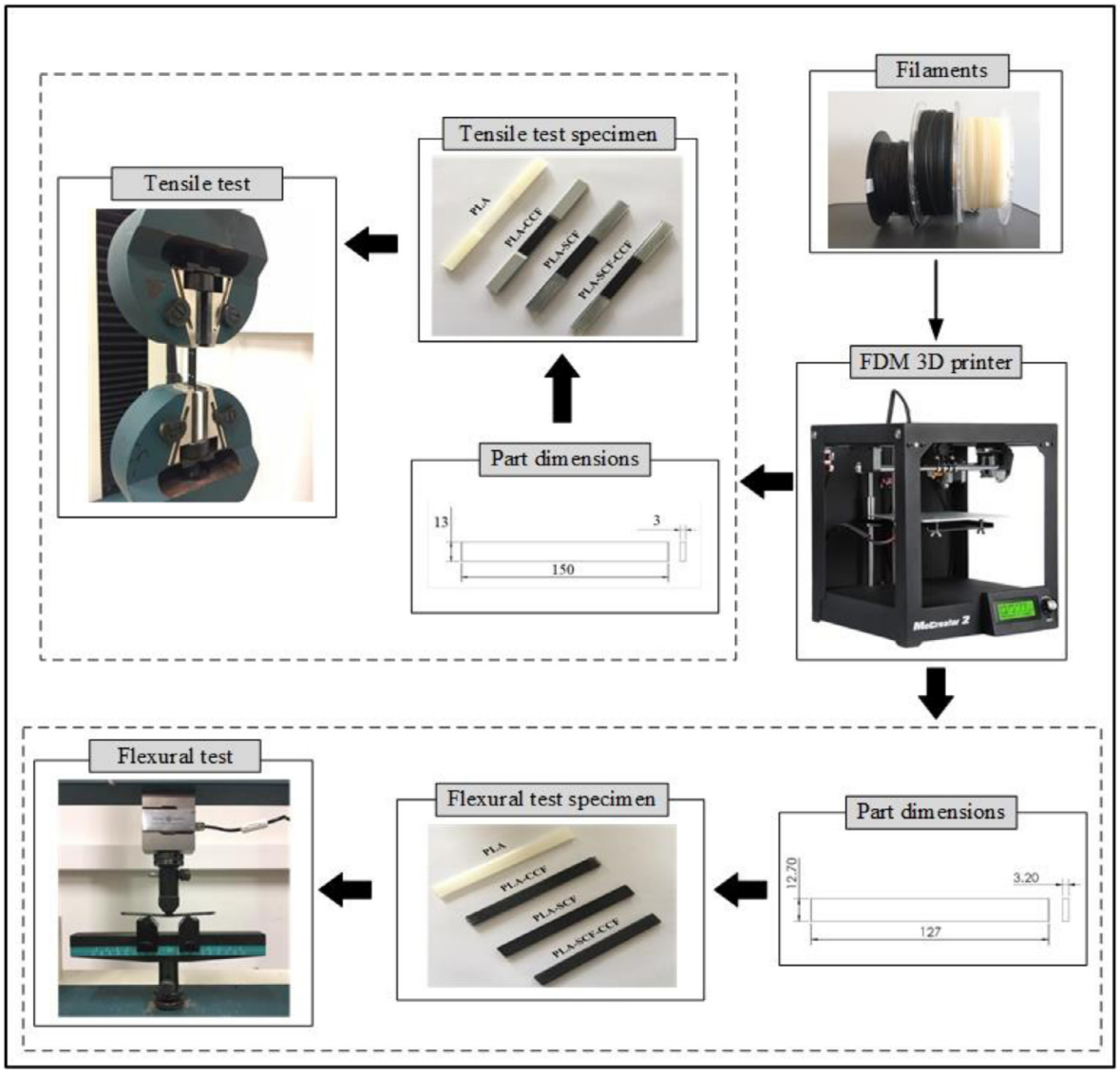

Fig. 2. Samples fabrication and testing process for the experiment.

strain values at the predetermined points on the load deflection curve. All the averages dimensions of 3D printed specimens used to perform mechanical testing are provided in Table 2.

2.4. Fracture interface of the specimens

Fracture interface of the specimens were observed after performing the mechanical testing using optical microscope (Nikon eclipse LV100ND) equipped with high definition color camera (Nikon DS-Ri2). The imaging software (NIS Elements 4.5.1.00) was used to prepare and process the data at 5x magnification to study the interfaces between the deposited lines as well as separated and fractured fibers in matrix after performing the tensile and flexural test. One specimen was chosen among the 5 tested samples to study the fracture interface.

3. Experimental results and discussions

3.1. Observation of prepared impregnated carbon fiber

After the impregnation process of carbon fiber, the impregnated carbon fiber tow was analyzed using optical microscope. Fig. 3(a) shows the optical micrograph of cross-section of the impregnated carbon fiber. From the cross-section view, the carbon fiber and PLA can clearly be observed with the presence of some air voids. The cross section of carbon fiber tow is of irregular geometric shape. The irregular shape is caused due to the impregnation process and cutting procedure of carbon fiber. During cutting procedure, the pressure deforms matrix material and change geometry from circular to elliptical shape. In the Fig. 3(b) the full-length micrograph view of impregnated carbon fiber is presented, which shows the smooth and uniform distribution of the plastic over the carbon fiber tow. Concentration of solution has high influence on the quality of carbon fiber tow. Increasing the concentration of the plastic solution allow to decrease the amount of air voids in impregnated carbon fiber tow [28]. Furthermore, the adhesion between carbon fiber impregnated with the matrix material can also be seen. The mechanical properties of carbon fiber impregnated with different concentration of solutions and its effect have been studied and showed that carbon fiber impregnated with 10% wt. solution provides the best result [28].

3.2. Tensile test response of CFRPC

The tensile test was performed to compare the tensile properties of the specimens printed for each group (PLA, PLA-CCF, PLA-SCF, PLA-SCF-CCF). Fig. 4 shows the fractured tested samples after perform-

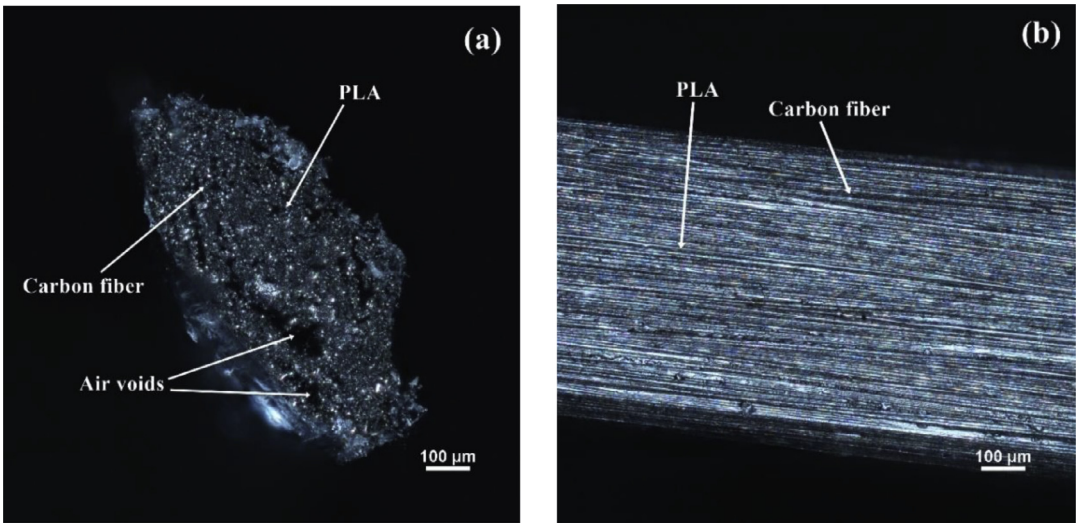

Fig. 3. The optical micrographs of the impregnated carbon fiber (a) cross-section (b) full-length.

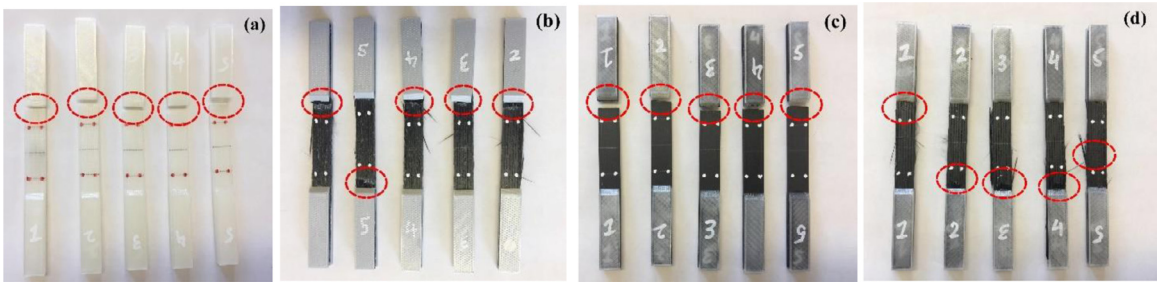

Fig. 4. Fractured samples after performing tensile testing (a) PLA (b) PLA-CCF (c) PLA-SCF (d) PLA-SCF-CCF.

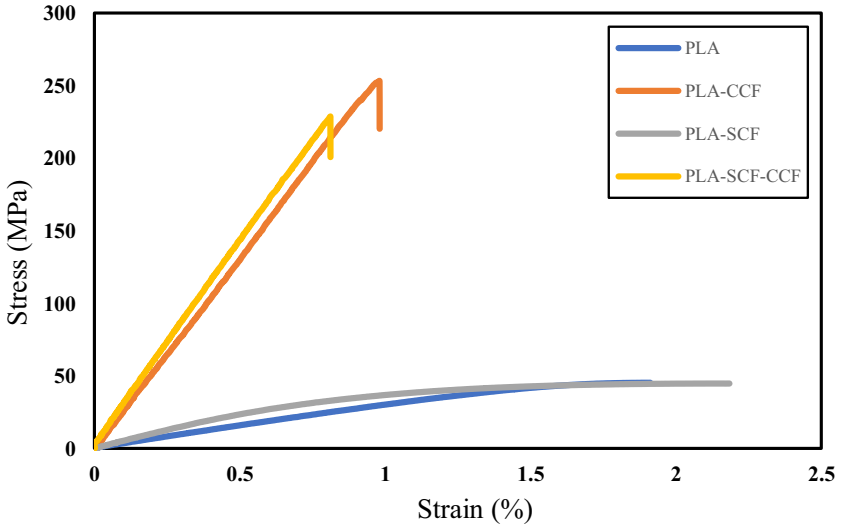

Fig. 5. Average stress–strain curve for the tensile samples.

ing tensile test of each group. Typical tensile stress-strain curves of the best representing curve from each group are presented in Fig. 5. Selection was made according to results i.e. curve which represent average tensile strength results from each group is presented in the figure.

From the stress-strain curves, it can be seen that the PLA-CCF attained the maximum value of ultimate tensile strength (UTS) followed by PLA-SCF-CCF, PLA-SCF and PLA, respectively. The tensile properties (including tensile strength, Young's Modulus and ductility) for each group are shown in Fig. 6. Bar graph plots were used to express the data of tensile properties. The mean values in bar plots were used to illustrate the trends of each printed group specimens with the range of their result effects on the tensile properties.

According to ASTM D3039, specimens printed with PLA-SCF showed the Grip-at tab-top (GAT) failure mode. While, the specimens printed with PLA-CCF and PLA-SCF-CCF shows the Lateral-at tab-top (LAT) failure mode (Fig. 4). The gripping pressure, specimen geometry, tab material affect the tensile strength of the specimens under the same test conditions [31] and different failure modes can also be observed, as in case, specimens printed with CCF showed similar mode of failure.

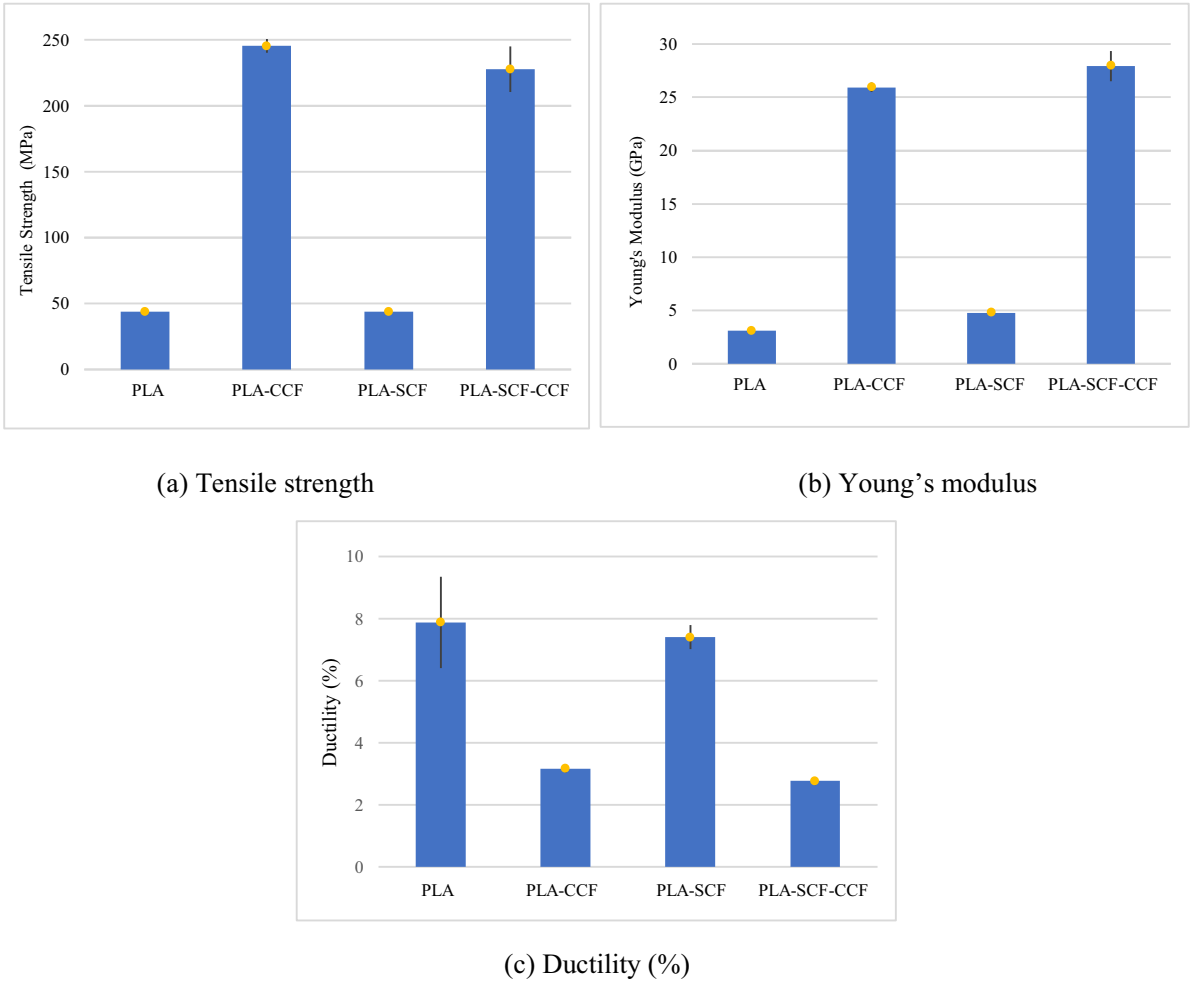

(a) Tensile strength

(b) Young's modulus

(c) Ductility (%)

Fig. 6. Results of tensile properties of 3D printed samples.

Table 3
Results of mechanical properties measured.

Specimens	Tensile Properties Tensile strength (MPa)	Young's modulus (GPa)	Ductility (%)	Flexural Properties Flexural stress (MPa)	Flexural modulus (GPa)
PLA	43.83 ± 2.39	3.09 ± 0.05	7.87 ± 1.47	83.18 ± 3.22	3.067 ± 0.29
PLA-CCF	245.40 ± 0.14	25.94 ± 0.47	3.16 ± 0.14	168.88 ± 5.17	10.63 ± 0.59
PLA-SCF	43.75 ± 0.39	4.79 ± 0.08	7.39 ± 0.39	76.33 ± 1.21	4.52 ± 0.11
PLA-SCF-CCF	227.56 ± 0.13	27.93 ± 1.40	2.76 ± 0.13	116.75 ± 13.3	10.85 ± 1.51

Table 3 shows the results of tensile properties measured from tensile testing.

3.2.1. Tensile strength

The tensile strength of the 3D printed specimens of each group is shown in Fig. 6(a). From the bar graph plot, it can be seen that the PLA-SCF attained the smallest average tensile strength value of 43.75 MPa. PLA has tensile strength value of 43.83 MPa (almost the same that of PLA-SCF). PLA-SCF-CCF showed the average tensile strength value of 227.56 MPa. The largest mean value of 245.40 MPa could be found in PLA-CCF group. PLA printed with impregnated CCF shows the highest tensile strength, about 6 times more compared to PLA and PLA-SCF, and even more strength compared to PLA-SCF printed with CCF, showed tensile strength, increased by 460% compared to pure PLA and PLA-SCF specimens and 7.84% compared to PLA-SCF-CCF specimens. Pure PLA showed similar strength result as provided by the producer, while in case of PLA-SCF, lower strength can be observed compared to strength mentioned by the producer. This is due to different selection of printing parameters and also weak interfacial bonding between the layers. The strength provided by the XT-CF20 producer was for the molded samples. In comparison to previous result [29], PLA-CCF showed increase in the tensile strength by 299.67%.

3.2.2. Young's modulus

The results of young's Modulus for each set of groups is shown in Fig. 6(b). The trend of results changed, as the highest mean Young's Modulus value of 27.93 GPa can be found in the PLA-SCF-CCF, followed by PLA-CCF, PLA-SCF and PLA having an average young's Modulus values of 25.94 GPa, 4.79 GPa and 3.09 GPa, respectively. The results indicated that by increasing the content of fibers in the matrix will increase the Young's Modulus value. The similar trend could also be observed [22] that increases the young's Modulus value up to certain level of content of fibers in the matrix.

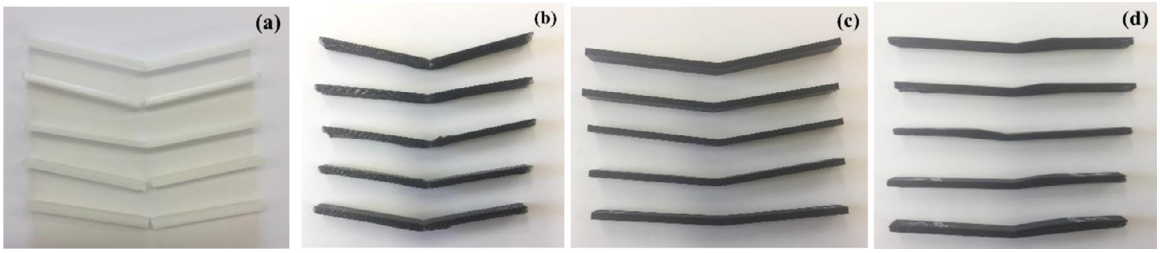

Fig. 7. Fractured samples after performing flexural testing (a) PLA (b) PLA-CCF (c) PLA-SCF (d) PLA-SCF-CCF.

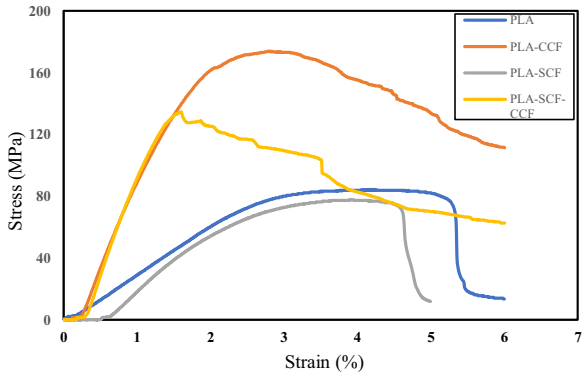

Fig. 8. Average stress–strain curve for the flexural samples.

3.2.3. Ductility

Fig. 6(c) shows the results of ductility measured from the tensile test results. From the result, it can be observed that the pure PLA has the highest mean ductility of 7.87%. PLA-SCF attained the average ductility value of 7.39%. While, PLA-CCF and PLA-SCF-CCF had average ductility values of 3.16% and 2.76%, respectively. PLA showed high standard deviation value due to presence of high deformation in strain values of the specimens. The ductility results indicated that by increasing the content of reinforcement fibers in the composite will tend to decrease in ductility [22].

3.3. Flexural test response of CFRPC

Flexural test was conducted to get the flexural properties of the specimens printed for each group (PLA, PLA-CCF, PLA-SCF, PLA-SCF-CCF). Fig. 7 shows the fractured tested samples after performing the flexural test. According to the ASTM D790 standard, flexural test would only be valid, if the maximum strain in the outer region of the specimen breakage occurred within the 5% strain limit. In this study, all the specimens breakage did not occur beyond the 5% strain limit. Typical flexural stress-strain curves of all the specimens for each group is demonstrated in Fig. 8. The curves were selected from the result of each groups. Selection was made according results i.e. curve which represent average flexural strength results from each group is presented in the Fig.. From the stress-strain curve, it can be seen that PLA printed with CCF showed the maximum value of stress followed by PLA-SCF-CCF, PLA and PLA-SCF, respectively. Comparison of flexural properties (flexural stress and flexural modulus) among each set of CFRPCs group are shown in Fig. 9. Table 3 shows the results of flexural properties values measured from flexural testing. Increasing layer thickness decreases the carbon fiber content, thus further reduced the flexural strength of the CFRPC [25]. The PLA-SCF-CCF showed a sudden breakage and decrease in the stress value in a stress-strain curve and also high standard deviation values in both the cases (flexural stress and flexural modulus); this fluctuation in the results may occurred during the test due to poor interfacial bonding between the layers of the specimen [32] that can cause such variations.

During the flexural testing, the PLA, PLA-CCF, PLA-SCF specimens when undergoes bending, fracture occured at the applied load (Fig. 7a–c). In case of PLA-SCF printed with CCF, when undergoes bending, delamination occured instead of breakage towards the sides of the applied load at the center and the layers of the fiber separated and created gaps between the printed layers (Fig. 7d).

3.3.1. Flexural stress

The flexural stress of the 3D printed specimens of each group is shown in Fig. 9(a). From the bar graph plot, it can be seen that PLA-CCF showed the largest mean flexural stress value of 168.88 MPa. PLA-SCF printed with CCF had the mean flexural stress value of 116.75 MPa. While, PLA and PLA-SCF showed the average flexural stress values of 83.18 MPa and 76.33 MPa, respectively. PLA printed with CCF showed highest flexural stress, increased by 121%, 103% and 44.6%, respectively, as compared with PLA-SCF, pure PLA and PLA-SCF-CCF specimen. The trend also shows that the flexural stress rises by increasing the content of CCF in the composite [11]. The lower flexural stress compared to tensile strength indicateed there may be concerns with the quality of the printed specimen, as higher flexural stress is predictable for high excellence fiber composites [33]. In comparison to previously achieved result [29], the flexural strength is increased by 11.03%.

3.3.2. Flexural modulus

Fig. 9(b) shows the result of flexural modulus for each set of groups. The highest mean flexural modulus value of 10.85 GPa can be found in the PLA-SCF printed with CCF, as same trend can be seen in case of tensile test. PLA-CCF, PLA-SCF and pure PLA showed the average flexural modulus values of 10.63 GPa, 4.52 GPa and 3.06 GPa, respectively. The flexural modulus results also indicated that by increasing the fibers reinforcement content in the matrix, will increase the flexural modulus of the composite [22].

3.4. Fracture interface observation after mechanical testing.

Based on experimental results of tensile and flexural tests, PLA-CCF and PLA-SCF-CCF showed better strength results, compared to PLA and PLA-SCF. Therefore, it was decided to study the fracture interface of the 3D printed samples to observe the deformation behavior and how the fracture occurs during the mechanical testing. To investigate such occurrence, the fracture interface of CCPRPC specimens for each group was observed by optical microscope. One specimen from each group best reflecting failure mode was selected to study such results. Optical micrographs were used to explore the specimen interfacial adhesion between the CCF and PLA thermoplastic matrix.

Optical micrographs of specimens from each group after performing tensile test are shown in Fig. 10. It can be seen that the pure PLA specimen showed the rupture at the interface, showing no such adhesion and each layer is separated from each other. The same result can be observed in case of PLA-SCF, which shows rough surface, due to presence

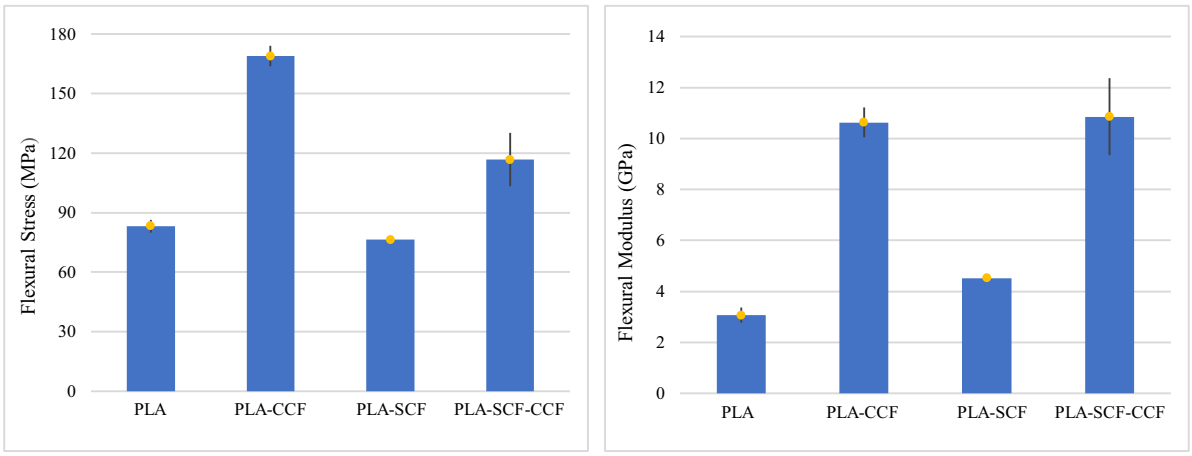

(a) Flexural stress (b) Flexural modulus

Fig. 9. Results of flexural properties of 3D printed samples.

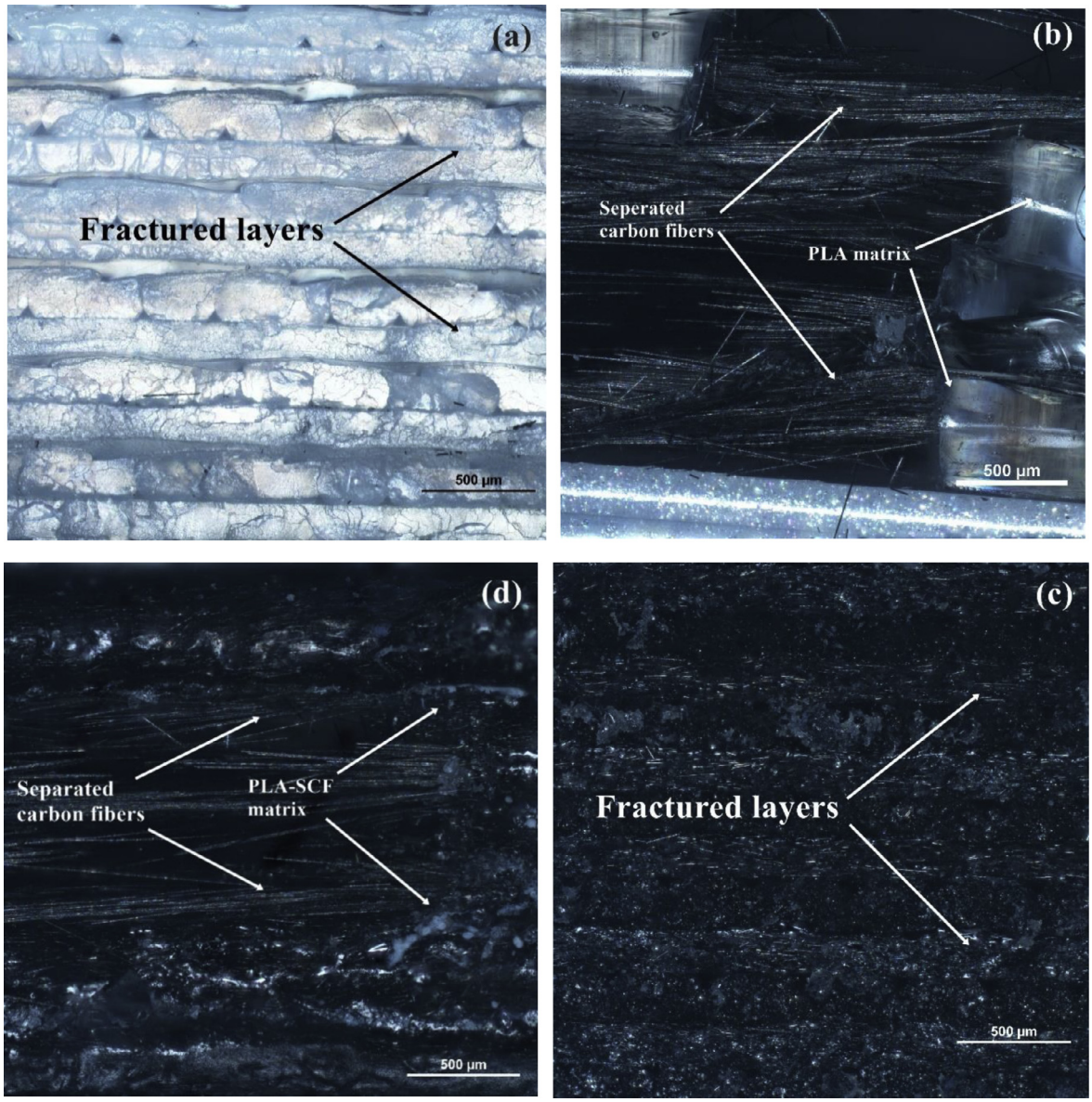

Fig. 10. The optical micrographs of fracture interface after performing tensile test of (a) PLA (b) PLA-CCF (c) PLA-SCF (d) PLA-SCF-CCF.

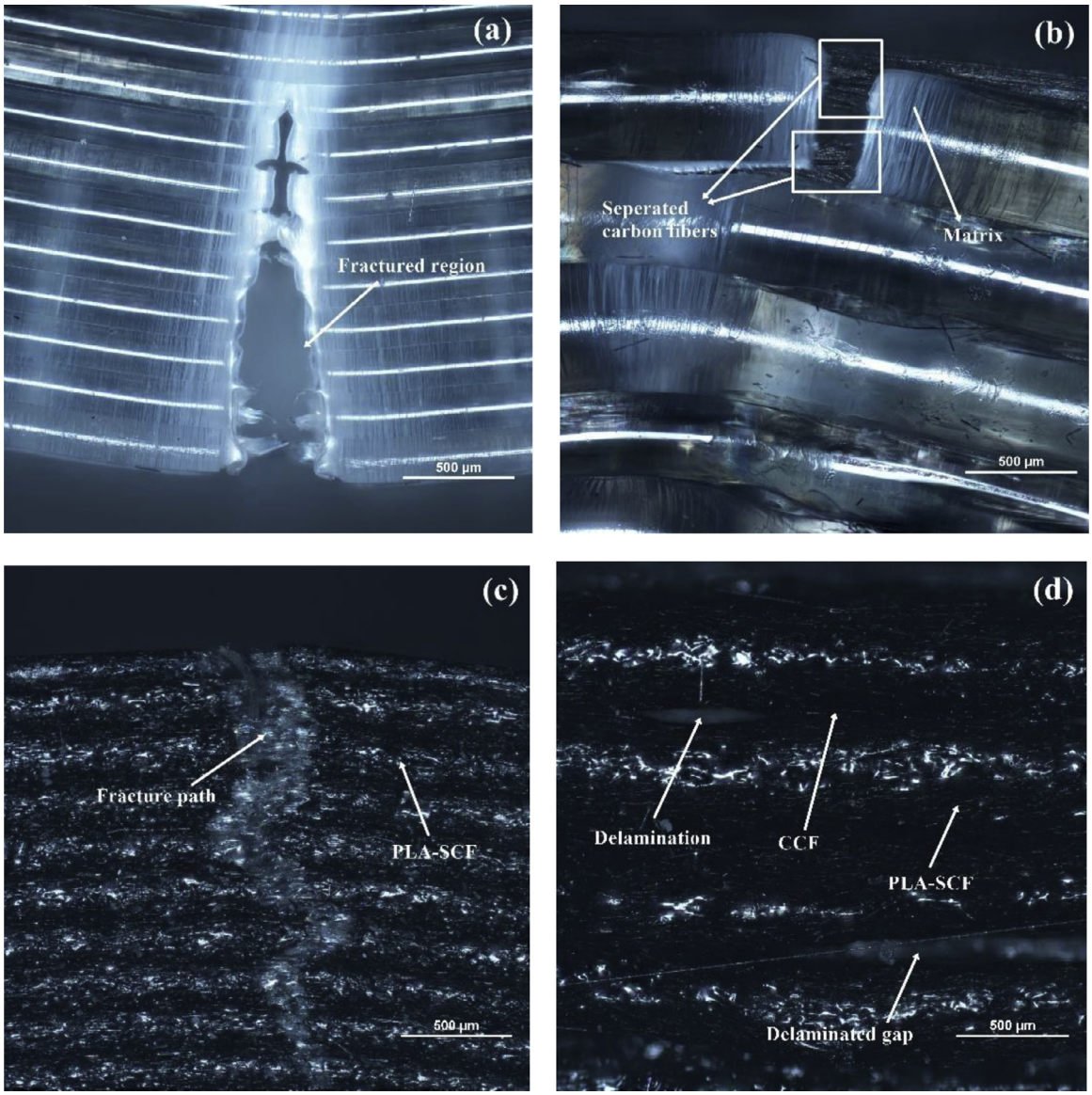

Fig. 11. The optical micrographs of fracture interface after performing flexural test of (a) PLA (b) PLA-CCF (c) PLA-SCF (d) PLA-SCF-CCF.

of chopped fibers and the rupture can be clearly seen as each 3D printed layer is detached after the test. Short fibres filament increases the stiffness but the strength of part increases is still limited as fibre pull out may occur before fibre breakage [34]. Separated CCF from the thermoplastic matrix can be observed in PLA-CCF, but still holds the fibers together with the matrix at various portion. Bonding between CCF and PLA-SCF can be seen after performing the test; CCF has created the gaps between the matrix, but the carbon fiber still holds within it, but separated and created the gaps, which indicates the poor adhesion between them. In both (PLA-CCF and PLA-SCF-CCF) cases, Fig. 10(b and d) shows that CCF composite parts can be used to support load during tension, compared to PLA and PLA-SCF, as the ruptured fibers in the fracture interface showed that the load was effectively transferred from the matrix to the fiber reinforcement for better properties. This can also be proved by better tensile strengths results.

Fig. 11 shows the optical micrographs of specimens after performing flexural testing. A clear fractured region can be observed in pure PLA, showed no such adhesion between the layers. PLA-SCF showed an irregular fractured path, but a better adhesion can be observed compare to pure PLA, due to presence of chopped carbon fibers, although a rough surface can be seen between 3D printed layers. The separated CCF can clearly be seen (Fig. 11b) after performing the test, but still holds the fibers together within matrix, which showed that the CCFRPC part structures can be used to support the load during the bending and the ruptured CCF in the fracture interface indicated that the load was effectively transferred from the PLA thermoplastic matrix to the carbon fibers to attain better mechanical properties. This can also be explained by the highest flexural stress among each group. Delaminated gaps were created during the test as it can clearly be seen in PLA-SCF-CCF specimen (Fig. 11d).

In case of PLA-SCF printed with CCF, when undergoes bending test, delamination occured instead of rupture as shown in Fig. 12. The printed layers of the specimen separated and created gaps between them towards the sides of the applied load. The CCF displaced from their position upon load that created bond with the PLA-SCF matrix. This type of behavior shows that this is due to weak an insufficient bonding between the printed layers and bonding with the matrix, hence showed poor adhesion between them.

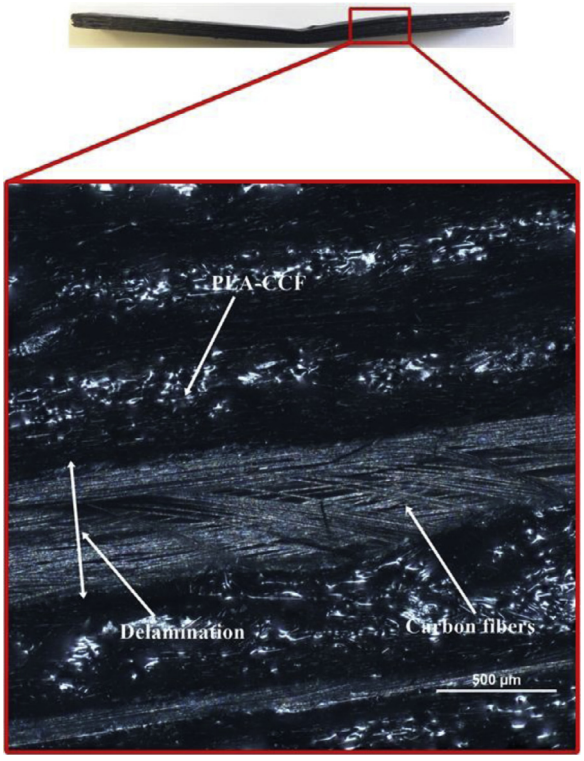

Fig. 12. The optical micrograph of the delamination caused in PLA-SCF-CCF 3D printed sample during flexural test.

4. Conclusion

Following conclusions were drawn from this study.

1 CCF reinforced PLA composite showed highest tensile strength and Young's Modulus of 245.40 MPa and 27.93 GPa, respectively. The PLA-CCF specimen's strength increased by 460% compared to pure PLA and PLA-SCF specimens and 7.84% compared to PLA-SCF-CCF specimens. Moreover, result proved that by increasing the fiber's reinforcement content in the matrix will increase the Young's Modulus value, while ductility tends to decrease.

2 PLA-CCF specimens showed the largest mean flexural stress value of 168.88 MPa, compared to other sets of groups and increased by 121%, 103% and 44.6%, compared to PLA-SCF, pure PLA and PLA-SCF-CCF specimen, respectively. While, PLA-SCF printed with CCF had the highest mean flexural modulus value of 10.85 GPa and resulted that by increasing the fibers reinforcement content in the matrix, will increase the flexural modulus of the composite.

3 Optical micrograph of the cross-section of impregnated carbon fiber confirms the existence of the resin and CCF with the presence of some air void contents in it. Fracture interfaces after performing tensile testing presented that the pure PLA and PLA-SCF specimens showed no such interfacial bonding between the separated layers, while the specimen printed with CCF indicated that composite parts can be used to support load during tension as the ruptured fibers in the fracture interface showed that the load was effectively transferred from the matrix.

4 Fracture interface's optical micrographs after performing flexural test presented a clear fractured region in pure PLA and PLA-SCF. PLA-CCF fractured region still holds the fibers together within matrix, resulted CCFRPC part structures can be used to support the load during the bending. While, PLA-SCF printed with CCF, when undergoes bending delamination occurs instead of rupture at the applied load, representing poor interfacial bond between the matrix and fiber.

Declaration of Competing Interest

None.

Acknowledgment

This research was funded by a grant (No. S-M-ERA.NET-17-4) (project: Additive Manufacturing of Continuous Fibers Reinforced Polymer Composite Materials for High Performance Structural Applications, acronym: "3D-CFRP") from the Research Council of Lithuania.

References

[1] ASTM INTERNATIONAL, ASTM F2792-12a, in: Rapid Manuf. Assoc., 2013, pp. 1–3, doi:10.1520/F2792-12A.2.
[2] X Wang, M Jiang, Z Zhou, J Gou, D. Hui, 3D printing of polymer matrix composites: a review and prospective, Compos. Part B Eng. 110 (2017) 442–458, doi:10.1016/j.compositesb.2016.11.034.
[3] A El Moumen, M Tarfaoui, K. Lafdi, Additive manufacturing of polymer composites: processing and modeling approaches, Compos. Part B Eng. 171 (2019) 166–182, doi:10.1016/j.compositesb.2019.04.029.
[4] P Parandoush, D. Lin, A review on additive manufacturing of polymer-fiber composites, Compos. Struct. 182 (2017) 36–53, doi:10.1016/j.compstruct.2017.08.088.
[5] AN Dickson, JN Barry, KA McDonnell, DP. Dowling, Fabrication of continuous carbon, glass and Kevlar fibre reinforced polymer composites using additive manufacturing, Addit. Manuf. 16 (2017) 146–152, doi:10.1016/j.addma.2017.06.004.
[6] W Akram, AF Rafique, N Maqsood, A Khan, S Badshah, RU. Khan, Characterization of PTFE film on 316L stainless steel deposited through spin coating and its anticorrosion performance in multi acidic mediums, Materials 13 (2020), doi:10.3390/ma13020388.
[7] C Capela, SE Oliveira, JAM. Ferreira, Fatigue behavior of short carbon fiber reinforced epoxy composites, Compos. Part B Eng. 164 (2019) 191–197, doi:10.1016/j.compositesb.2018.11.035.
[8] O Ivanova, C Williams, T. Campbell, Additive manufacturing (AM) and nanotechnology: promises and challenges, Rapid Prototype J. 19 (2013) 353–364, doi:10.1108/RPJ-12-2011-0127.
[9] N Maqsood, A Khan, MK Alamgir, SA Shah, M. Fahad, PTFE thin film coating on 316L stainless steel for corrosion protection in acidic environment, J. Eng. Appl. Sci. 36 (2017) 183–190.
[10] S Chakraborty, MC. Biswas, 3D printing technology of polymer-fiber composites in textile and fashion industry: a potential roadmap of concept to consumer, Compos. Struct. 248 (2020) 112562, doi:10.1016/j.compstruct.2020.112562.
[11] T Yu, Z Zhang, S Song, Y Bai, D. Wu, Tensile and flexural behaviors of additively manufactured continuous carbon fiber-reinforced polymer composites, Compos. Struct. 225 (2019) 111147, doi:10.1016/j.compstruct.2019.111147.
[12] P Bettini, G Alitta, G Sala, L. Di Landro, Fused deposition technique for continuous fiber reinforced thermoplastic, J. Mater. Eng. Perform. 26 (2017) 843–848, doi:10.1007/s11665-016-2459-8.
[13] Adrian P Mouritz, Introduction to Aerospace Materials, first ed., Woodhead Publishing Ltd, Cambridge, England, 2012.
[14] E Zappino, M Filippi, A Pagani, M Petiti, E. Carrera, Experimental and numerical analysis of 3D printed open-hole plates reinforced with carbon fibers, Compos. Part C Open Access 2 (2020) 100007, doi:10.1016/j.jcomc.2020.100007.
[15] SMF Kabir, K Mathur, AFM. Seyam, A critical review on 3D printed continuous fiber-reinforced composites: history, mechanism, materials and properties, Compos. Struct. 232 (2020) 111476, doi:10.1016/j.compstruct.2019.111476.
[16] Chua Chee Kai, CSL Kah Fai Leong, Rapid Prototyping: Principles and Applications, World Scientific Publishing, 2003.
[17] JM Chacón, MA Caminero, PJ Núñez, E García-Plaza, I García-Moreno, JM. Reverte, Additive manufacturing of continuous fibre reinforced thermoplastic composites using fused deposition modelling: effect of process parameters on mechanical properties, Compos. Sci. Technol. 181 (2019) 107688, doi:10.1016/j.compscitech.2019.107688.
[18] Y Nakagawa, Mori K ichiro, T Maeno, 3D printing of carbon fibre-reinforced plastic parts, Int. J. Adv. Manuf. Technol. 91 (2017) 2811–2817, doi:10.1007/s00170-016-9891-7.
[19] J Justo, L Távara, L García-Guzmán, F. París, Characterization of 3D printed long fibre reinforced composites, Compos. Struct. 185 (2018) 537–548, doi:10.1016/j.compstruct.2017.11.052.
[20] N Maqsood, M.A Rimasauskas, Review on development and manufacturing of polymer matrix composites using 3D printing technologies, in: 9th Int. Sci. Conf. Defensive Technol. - OTEH, 2020, pp. 462–468.
[21] DA Türk, F Brenni, M Zogg, M. Meboldt, Mechanical characterization of 3D printed polymers for fiber reinforced polymers processing, Mater. Des. 118 (2017) 256–265, doi:10.1016/j.matdes.2017.01.050.
[22] F Ning, W Cong, J Qiu, J Wei, S. Wang, Additive manufacturing of carbon fiber reinforced thermoplastic composites using fused deposition modeling, Compos. Part B Eng. 80 (2015) 369–378, doi:10.1016/j.compositesb.2015.06.013.
[23] LJ Love, V Kunc, O Rios, CE Duty, AM Elliott, BK Post, et al., The importance of carbon fiber to polymer additive manufacturing, J. Mater. Res. 29 (2014) 1893–1898, doi:10.1557/jmr.2014.212.

[24] HL Tekinalp, V Kunc, GM Velez-Garcia, CE Duty, LJ Love, AK Naskar, et al., Highly oriented carbon fiber-polymer composites via additive manufacturing, Compos. Sci. Technol. 105 (2014) 144–150, doi:10.1016/j.compscitech.2014.10.009.
[25] X Tian, T Liu, C Yang, Q Wang, D. Li, Interface and performance of 3D printed continuous carbon fiber reinforced PLA composites, Compos. Part A Appl. Sci. Manuf. 88 (2016) 198–205, doi:10.1016/j.compositesa.2016.05.032.
[26] C Yang, X Tian, T Liu, Y Cao, D. Li, 3D printing for continuous fiber reinforced thermoplastic composites: mechanism and performance, Rapid Prototype J. 23 (2017) 209–215, doi:10.1108/RPJ-08-2015-0098.
[27] Z Hou, X Tian, J Zhang, L Zhe, Z Zheng, D Li, et al., Design and 3D printing of continuous fiber reinforced heterogeneous composites, Compos. Struct. 237 (2020) 111945, doi:10.1016/j.compstruct.2020.111945.
[28] M Rimašauskas, T Kuncius, R. Rimašauskienė, Processing of carbon fiber for 3D printed continuous composite structures, Mater. Manuf. Process. 34 (2019) 1528–1536, doi:10.1080/10426914.2019.1655152.
[29] M Heidari-Rarani, M Rafiee-Afarani, AM. Zahedi, Mechanical characterization of FDM 3D printing of continuous carbon fiber reinforced PLA composites, Compos. Part B Eng. 175 (2019) 107147, doi:10.1016/j.compositesb.2019.107147.
[30] Toray Composite Materials America. T300 standard modulus carbon fibers. 2018. https://doi.org/10.2115/fiber.66.p_184.
[31] G Belingardi, DS Paolino, EG. Koricho, Investigation of influence of tab types on tensile strength of E-glass/epoxy fiber reinforced composite materials, Procedia Eng. 10 (2011) 3279–3284, doi:10.1016/j.proeng.2011.04.541.
[32] M Nebe, T Schmack, T Schaefer, F. Walther, Composites Part C: Open Access Experimental and numerical investigation on the impact response of CFRP under 3-point-bending, Compos. Part C Open Access 4 (2021) 100079, doi:10.1016/j.jcomc.2020.100079.
[33] MR. Wisnom, The relationship between tensile and flexural strength of unidirectional composites, J. Compos. Mater. 26 (1992) 1173–1180, doi:10.1177/002199839202600805.
[34] LG Blok, ML Longana, H Yu, BKS. Woods, An investigation into 3D printing of fibre reinforced thermoplastic composites, Addit. Manuf. 22 (2018) 176–186, doi:10.1016/j.addma.2018.04.039.